Effect of Multi-axial Stress on the Life of Creep Crack Growth for Welded Joint of P92 Steel

R. Sugiura[1], A. T. Yokobori Jr. [1], K. Suzuki[1], M. Tabuchi[2].
[1]*Department of Nanomechanics, Graduate School of Engineering, Tohoku University, Sendai, Japan.*
[2]*National Institute for Materials Science, Tsukuba, Japan.*

1. Introduction

In industrial components operating at high temperatures, although the uni-axial external tensile load is applied, local multi-axial stress field is caused due to the locality of stress field such as plastic constraint, which is related to the structural brittleness. In previous paper, using a round bar specimen with a circular notch which causes the local multi-axial stress field due to the plastic constraint, the effect of local multi-axial stress on the creep crack growth rate has been investigated for creep-ductile and brittle materials such as Cr-Mo-V and W-added 12Cr steels[1,2)]. On the basis of these resluts, the concept of structural brittleness was proposed[1,2)]. Furthermore, in weldments, it has been shown that the local multi-axial stresses are also caused due to the plastic constraint induced by a decrease in hardness of the heat affected zone as compared with that of a base metal and weld metal by conducting the creep crack growth tests using the welded joint of C(T) specimen and finite element analyses[3,4)]. Under these situations, it is important to conduct the characterizations of the creep crack growth rate and its life under the multi-axial stress field to predict the life of creep crack growth[5)].

However, since the creep crack growth under the local multi-axial stress occurs in brittle manner[1-4)], it is considered that the construction of the predictive law of the fracture life focusing on the creep crack growth is difficult.

In the present paper, using the master curve[6)] of creep deformation based on the similarity law of creep deformation plotted against the normalized time of stress application, the effects of local multi-axial stresses on the law of load line displacement are discussed. Furthermore, three-dimensional elastic-plastic creep finite element analyses are conducted to clarify the effect of local multi-axial stress of welded joint on the load line displacement law and creep ductility. The proposed master curve of creep deformation represented by normalized time t/t_f enables us to find out the existence of a similarity law of creep deformation and the dependence of the characteristics of creep deformation. Furthermore, it was found to be capable of characterizing the creep ductility[7)].

2. Materials and specimen

The material used is the W-added 9%Cr ferritic heat resistant steel [8, 9)], ASME Code Case 2179/ASTM A335 P92, which is used for a boiler material. The chemical composition of this material is shown in Table 1. The material is normalized at a temperature of 1070 ^{o}C for 2 hr and tempered at a temperature of 780 ^{o}C for 2 hr. The welded joint was fabricated by Gas Tungsten Arc (GTA) welding and the post weld heat treatment (PWHT) was carried out at a

temperature of 740 ^{o}C for 4 hr. The process parameters of multi-layer GTA welding are given in Table 2[10].

The specimens used are a circular notched round bar specimen for creep crack growth test under the local multi-axial stress field[11] and a standardized C(T) pre-cracked specimen with side-groove[12]. The geometry and size of a circular notched specimen and a C(T) specimen with side-groove are shown in Figs. 1 and 2, respectively. In both of the specimens, the sites of base metal (BM), heat affected zone (HAZ) and weld metal (WM) are also shown in Figs. 1 and 2, respectively.

Table 1 Chemical composition of P92 in mass % (Bal. Fe)

C	Si	Mn	P	S	Cr
0.09	0.16	0.47	0.01	0.001	8.72
Mo	W	V	Nb	B	N
0.45	1.87	0.21	0.06	0.002	0.05

Table 2 Process parameters of multi-layer GTA welding

groove	preheating	welding current
single bevel 20°	>373K	200~250A
arc voltage	welding speed	multi-layer
10~10.5V	1.2~1.5mm/s	33~37pass

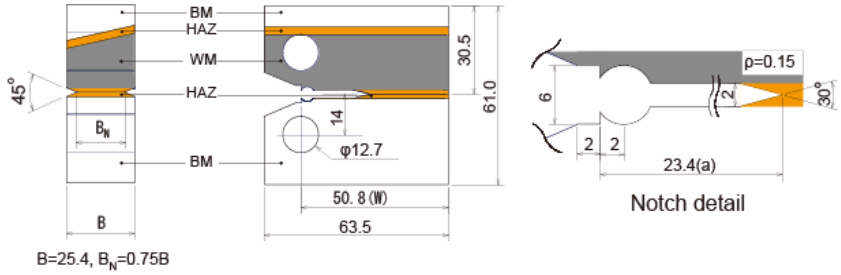

Fig. 1 Geometry and size of a C(T) specimen with side-grooves and the sites of base metal (BM), heat affected zone (HAZ) and weld metal (WM).

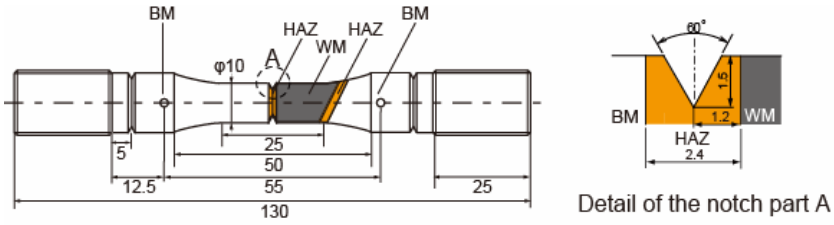

Fig. 2 Geometry and size of a circular notched specimen and the sites of base metal (BM), heat affected zone (HAZ) and weld metal (WM).

3. Experimental procedure

Crack growth tests were performed using a lever arm creep testing machine of Type RT-30 manufactured by TOSHIN KOGYO. The crack length and load line displacement were measured. The creep crack growth tests using C(T) specimens were conducted on the basis of ASTM E1457-07 and JSPS standard[12, 13]. The crack length from a tip of circular notch was measured by an electrical potential method[14, 15] using the modified Equation (1) [2].

$$a = 0.667 a_0 \exp\left[0.434 \frac{D}{\pi a} \cos^{-1}\left\langle \frac{\cosh(\pi y / D)}{\cosh\left\{ U / U_0 \cosh^{-1}\left[\cosh(\pi y / D) / \cos(\pi a_0 / D) \right] \right\}} \right\rangle \right] \quad (1)$$

where a is the length of crack (mm), a_0 is the initial crack length (mm), y is the half the distance between the output terminals (mm), U_0 is the initial voltage (μV), U is the actual value of the potential (μV), D is the diameter of specimen (mm).

The test temperatures were kept at a specified temperature with the precision of ± 2 ^{o}C. The experimental conditions are shown in figures of experimental results.

4. Experimental results and analyses

4.1 Characteristic of load line displacement

The characteristics of creep deformation are given by the relative non-dimensional load line displacement $\Delta\delta / \delta_0$, where $\Delta\delta$ and δ_0 are the load line displacement up to the current time and the initial notch opening value [The initial measured δ_0 for C(T) and circular notched specimens are 6 and 1.7 mm, respectively]. The relationship between $\Delta\delta / \delta_0$ and the normalized time t/t_f of base metal and welded joint of circular notched specimens is shown in Fig. 3, where t is the load application time and t_f is the creep crack growth life time for each specimen. In this figure, the data of base metal and welded joint of C(T) specimens are shown as data bands.

Figure 3 shows that in both of the specimens, the values of load line displacement for welded joint decrease as compared with those of base metal. Furthermore, with increase in temperature, the value of load line displacement for welded joint of circular notched specimens is found to increase.

In the next section, using the master curve[6] for creep deformation based on the similarity law of creep deformation against the normalized time of stress application, the effects of local multi-axial stress of welded joint and temperature on the law of load line displacement are discussed.

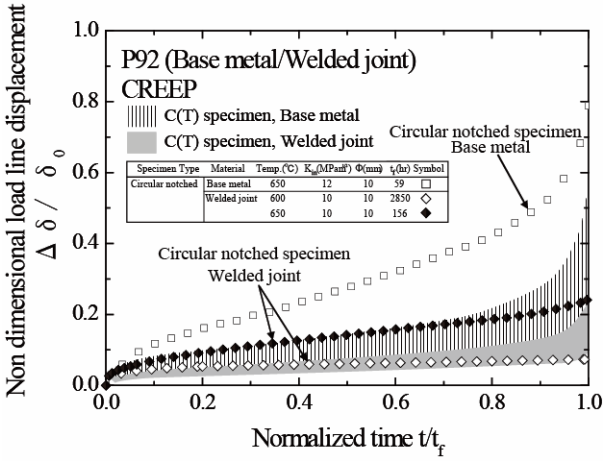

Fig. 3 Characteristic of load line displacement of welded joint and base metal for C(T) and circular notched specimens.

4.2 The law of load line displacement

Equation (2) has been proposed as the master curve for creep deformation of a cracked specimen[6] based on the similarity law of creep deformation. In this equation, normalized time t/t_f is used instead of stress application time t, which is different from the θ projection method[16]. This methodology enables us to predict the fracture life only if the present creep deformation and time of stress application t are known[6].

$$\frac{\Delta\delta}{\delta_0} = \alpha_1 + \alpha_2\left\{1-\exp(-\alpha_3\frac{t}{t_f})\right\} + \alpha_4\left\{\exp(\alpha_3\frac{t}{t_f})-1\right\} \quad (2)$$

where t is the time of stress application, t_f is the creep fracture time, α_i are constants (i=1~4).

The first term of equation (2) represents instantaneous elastic deformation, the second term represents transient creep deformation and the third term represents accelerating creep deformation. Using the non-linear least square method, the experimental characteristics of load line displacement represented by t/t_f were approximated by Equation (2) and each value of α_i (i=1~4) were determined[6]. This constitutive equation represented by normalized time t/t_f enables us to distinguish the existence of a similarity law for creep deformation and the dependence of temperature. Furthermore, it was found to be capable of characterizing the creep ductility[7].

The results calculated from Equation (2) are shown in Figs. 4-7. In Figs. 4-7, the analytical results represented by the solid lines are found to be in good agreement with the experimental results. The each values of α_i (i=1~4) obtained from Figs. 4-7 are shown in Table 3 and the relationship between the value of α_3, which represents the accelerating creep deformation related to the creep ductility, and temperature are shown in Fig. 8.

In Fig. 8, for C(T) specimens, the values of α_3 for base metal were found to be 7.31-7.66. The values of α_3 for welded joint were found to take constant, independently of temperature, and it is 8.08 which is larger than that of base metal. These values of α_3 for base metal and welded joint equal to the value of Ni based super-alloy which is creep-brittle material[7]. On the other hand, for circular notched specimens, the value of α_3 for base metal was found to be 4.93 which is smaller than those of C(T) specimens. The values of α_3 for welded joint were found to be 4.98 and 3.7 for 600 ^{o}C and 650 ^{o}C, respectively. This result shows that with decrease in temperature, the value of α_3 increases, which result in the dependence of temperature. In comparison the value of α_3 for welded joint with that fore base metal, α_3 of welded joint has a lower value due to the decrease in the load line displacement in the region of accelerating creep on Fig. 7, differently from the relationship between the α_3 of base metal and welded joint for C(T) specimens. However, in fact, a drastic increase of the load line displacement of welded joint in the region of accelerating creep was confirmed by the experiment. Therefore, for the circular notched specimen, the value of α_3 of welded joint will be larger than that of base metal and it needs further consideration. These values

of α_3 for base metal and welded joint for circular notched specimen mentioned above equal to the value of Cr-Mo-V steel which is creep-ductile material[6].

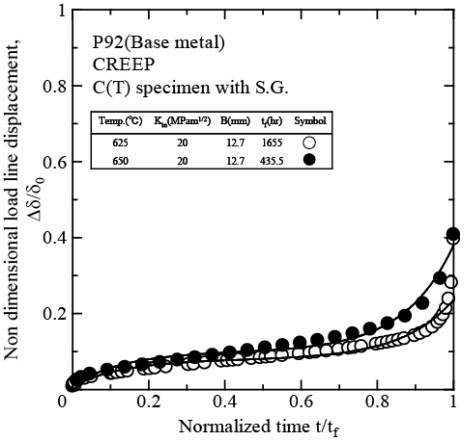

Fig.4 Experimental data for base metal of C(T) specimen and curve calculated from Eqn. (2).

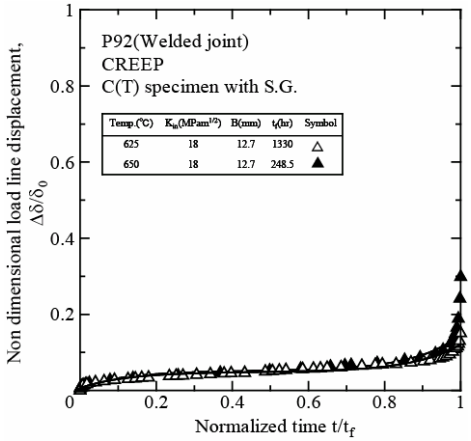

Fig.5 Experimental data for welded joint of C(T) specimen and curved calculated from Eqn. (2).

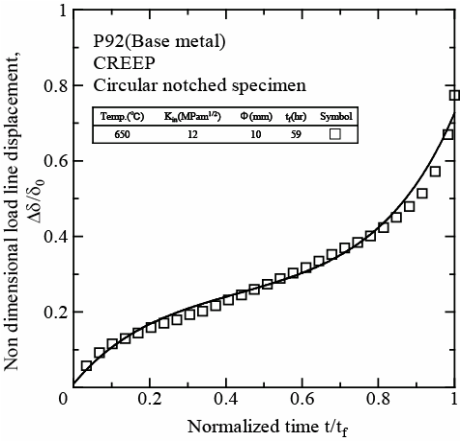

Fig.6 Experimental data for base metal of circular notched specimen and curve calculated from Eqn. (2).

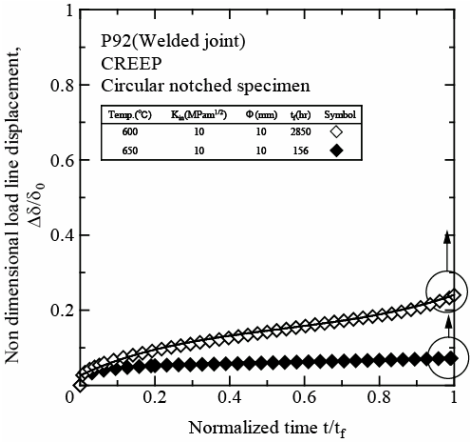

Fig.7 Experimental data for welded joint of circular notched specimen and curve calculated from Eqn. (2).

Table 3 The value of α_i(i=1~4)

Specimen	Material	Temp. °C	B, ϕ mm	K_{in} MPam$^{1/2}$	Symbol	α_1 $\times 10^{-3}$	α_2 $\times 10^{-2}$	α_3 $\times 10^{0}$	α_4 $\times 10^{-4}$
C(T) with S.G.	Base metal	625	12.7	20	○	8.99	6.96	7.31	1.05
		650	12.7	20	●	8.33	9.02	7.66	1.33
	Welded joint	625	12.7	18	△	6.72	4.19	8.08	0.23
		650	12.7	18	▲	8.08	4.37	8.08	0.29
Circular notched	Base metal	650	10	12	□	9.4	24.3	4.93	34.6
	Welded joint	600	10	10	◇	32.1	3.16	4.98	0.784
		650	10	10	◆	26	12.7	3.7	23.1

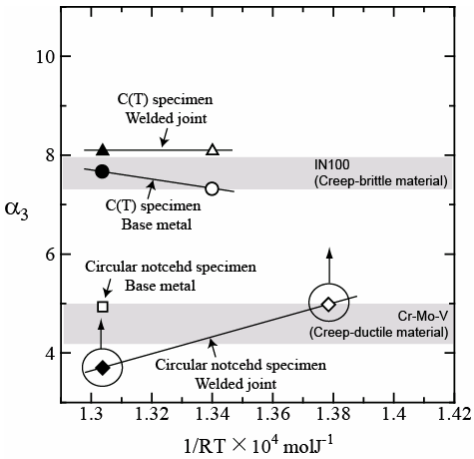

Fig.8 Relationship between α_3 and T

4.3 Estimation of creep ductility using *QL parameter**

In this section, on the basis of *QL** parameter[17,18], the estimation of creep ductility was conducted and it was compared with the previous experimental results of α_3 related to the characteristic of creep deformation.

The description of *QL** parameter[17,18] which has been proposed as a method of estimating the creep ductility, is shown as follows.

The *QL** parameter is represented by a combination of creep crack growth life derived from the *Q** concept and steady-state creep rate. The law of creep crack growth rate is given by Equation (3) based on the concept of *Q** parameter[19, 20].

$$\frac{da}{dt} = A\exp(Q^*) = A_g \sigma_g^{m_g} \exp\left(-\frac{\Delta H_g}{RT}\right) \tag{3}$$

where A and A_g are constants, σ_g is the term of gross stress (MPa), m_g is the exponent of the gross stress, ΔH_g is the activation energy (kJ/mol), R is the gas constant (=8.3145J/Kmol) and T is the absolute temperature (K).

By integrating Equation (3) from a_i (initial crack length in mm) to a_f (final crack length in mm), the life of creep crack growth t_f is given by Equation (4).

$$t_f = \frac{1}{A_g \sigma_g^{m_g} \exp\left(-\frac{\Delta H_g}{RT}\right)}(a_f - a_i) = \frac{1}{A^* \sigma_g^{m_g} \exp\left(-\frac{\Delta H_g}{RT}\right)} \tag{4}$$

where A^* is a constant($=A_g/(a_f-a_i)$).

The equation of the steady-state creep rate is given by Equation (5).

$$\dot{\varepsilon}_s = A_c \sigma_g^{m_c} \exp\left(-\frac{\Delta H_c}{RT}\right) \tag{5}$$

where A_c is a constant, m_c is the exponent of the gross stress and ΔH_c is the activation energy (kJ/mol)

By multiplying the Equations (4) and (5), *QL** is given by Equation (6) which concerns the creep ductility[17,18].

$$QL^* = t_f \dot{\varepsilon}_s = M \sigma_g^m \exp\left(-\frac{\Delta H}{RT}\right) \tag{6}$$

where M is a material constant depending on the creep ductility ($M=A_c/A^*$), $m=m_c-m_g$ and $\Delta H = \Delta H_c - \Delta H_g$.

Apparently, Equation (6) is in accord with the Monkman-Grant experimental law, however, it is noted that the right hand side of Equation (6) is a function of applied stress and temperature, depending on materials. For example, in Fig. 9, it can be seen that with decrease in the creep crack growth life and steady-state creep rate, the experimental data shift to the brittle region as creep ductility on the graph[17,18].

On the basis of *QL** concept mentioned above, the logarithm values of the creep crack growth life t_f are plotted against the logarithm values of the steady-state creep rate $\dot{\varepsilon}_s$ for base metal and welded joint for C(T) and circular notched specimens, as shown in Fig. 9. Figure 9 shows that, in both of C(T) and circular

notched specimens, the experimental characteristics of welded joint fall into a lower position as compared with those of base metal, which mean that the welded joint have a lower value of *QL** and a lower ductility. In comparison the experimental results of circular notched specimen with those of C(T) specimen, the creep ductility of circular notched specimen were found to increase as compared with those of C(T) specimens. This will be due to a smaller value of tri-axial factor *TF* for circular notched specimen around the notch tip as compared with that of C(T) specimen as shown in following section.

To compare the creep ductility mentioned above with the previous experimental results of α_3, the relationship between the *QL** and α_3 is shown in Fig. 10. Figure 10 shows that, with increase in the value of *QL**, the values of α_3 decrease. The values of α_3 were found to show the inverse correlation with the *QL**. For welded joint for circular notched specimens, the data marked by ◇ and ◆ in Fig. 10 deviate from the standard line due to a lower value of α_3. However, as mentioned in the previous section, α_3 of welded joint will have a large value due to a drastic increase of load line displacement confirmed by experiments.

In the next section, in order to investigate the effects of multi-axial stresses of welded joint and a circular notch on creep ductility and LLD law, three-dimensional elastic-plastic creep FEM analyses were conducted.

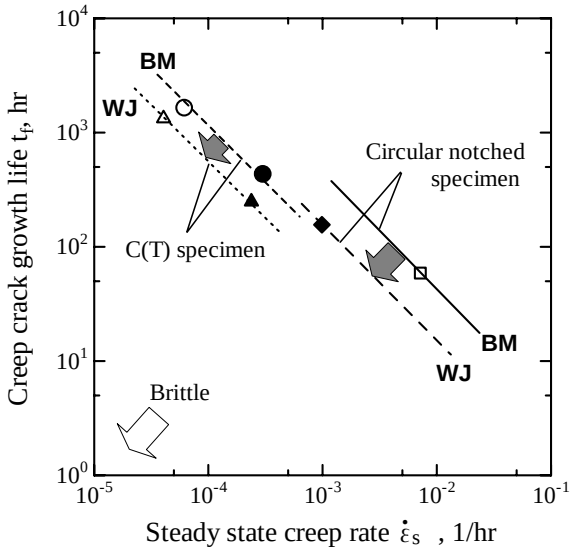

Fig.9 Relationship between creep crack growth life and steady state creep rate for base metal (BM) and welded joint (WJ) for C(T) and circular notched specimens.

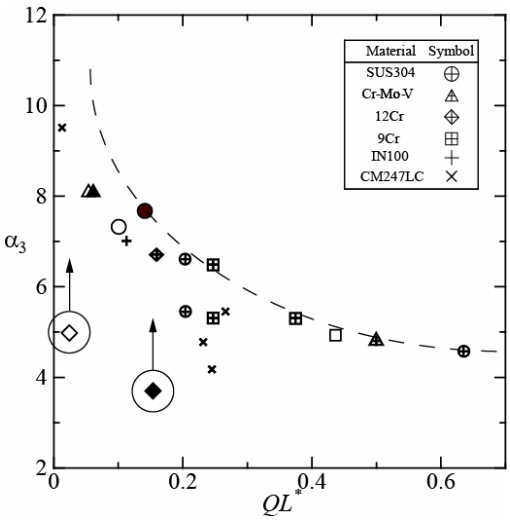

Fig.10 Relationship between the value of α_3 and QL*

4.4 Three-dimensional elastic-plastic creep finite element analysis

Three-dimensional analysis models of a circular notched specimen (ϕ =10mm, a_0=1.5mm) and a C(T) (W=50.8mm, B=25.4mm) specimen with side-groove (S.G.) are shown in Figs. 11 and 12. The sites of base metal, heat affected zone and weld metal both for C(T) and circlar notched specimens are shown in Figs. 13 and 14. The type of element used is 8-noded element for both models. For a C(T) specimen with S.G., the number of nodes and elements are 57142 and

51760, respectively. The size of smallest element at the crack tip is 0.1 mm in the heat affected zone. For a circular notched specimen, the number of nodes and elements are 11645 and 10268, respectively. The size of smallest element at the crack tip is 0.04 mm in the heat affected zone.

Three-dimensional elastic-plastic creep FEM analysis was conducted using MSC Marc/MSC Marc Mentat Ver. 2005 (Cyber Science Center, Tohoku University) and constitutive laws used were as follows.

The characteristic of workhardening for plastic deformation is approximated by Equation (7),

$$\sigma = c(a + \varepsilon_p)^{\alpha} , \tag{7}$$

where c, a and α are constants, ε_p is the plastic strain.

Creep strain rate is defined by Nortons law as follows,

$$\dot{\varepsilon} = A\sigma^{n} , \tag{8}$$

where $\dot{\varepsilon}$ is creep steady-state strain rate (1/hr), the values of A and n of Norton's law are shown in Table 4.

The stress tri-axiality factor TF is given by Equation (9),

$$TF = (\sigma_1 + \sigma_2 + \sigma_3)/\sigma_{eq} , \tag{9}$$

where σ_1, σ_2 and σ_3 are values of principle stress and σ_{eq} is Von Mises's equivalent stress.

The distributions of stress tri-axiality factor TF of base metal and welded joint for a circular notched specimen and C(T) specimens with side-grooves for W-added 9%Cr steel in the longitudinal direction in the vicinity of notch root were shown in Fig. 15.

Figure 15 shows that the values of stress tri-axiality factor TF of welded joint both of C(T) and circlar notched specimens are larger than those of base metal. This will be due to the multi-axial stress field induced by plastic constraint, caused by a decrease in hardness of the heat affected zone as compared with that of a base metal and weld metal. This analytical result mentioned above and the experimental results in the previous section are typical evidences. Furthermore, it can be seen that around the notch tip, the value of stress tri-axiality factor TF for a circular notched specimen is smaller than that of a C(T) specimen with S.G., which closely concerns the effect of multi-axial stress on creep ductility. That is, creep ductilty was found to be unified by the stress tri-axial factor TF near the crack tip.

Table 4 Creep properties of welded joint of P92.

	A ($MPa^{-n}h^{-1}$)	n
Fine grain HAZ	$8.30*10^{-13}$	3.68
Base metal	$3.77*10^{-19}$	6.71
Weld metal	$7.28*10^{-16}$	4.7

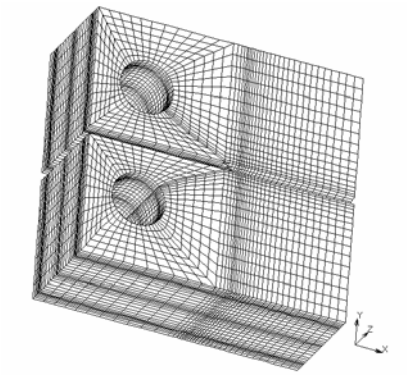

Fig. 11 Three-dimensional analysis model of a C(T) specimen with side-groove (W=50.8mm, B=25.4mm)

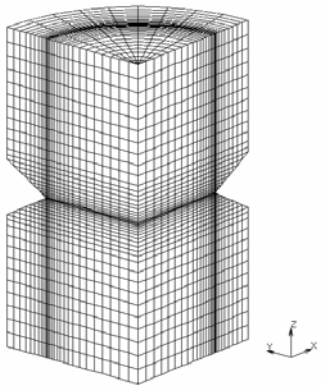

Fig. 12 Three-dimensional analysis model of a circular notched specimen (ϕ =10mm, a_0=1.5mm)

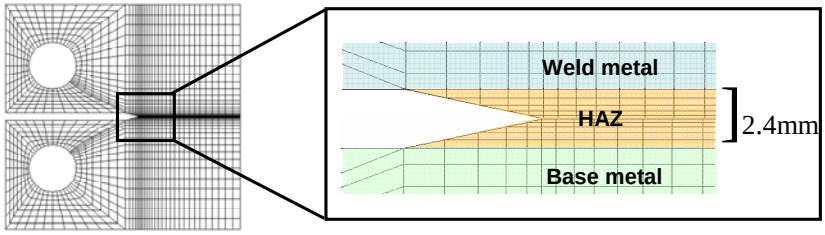

Fig. 13 The location of base metal, heat affected zone and weld metal for a C(T) specimen with S.G.

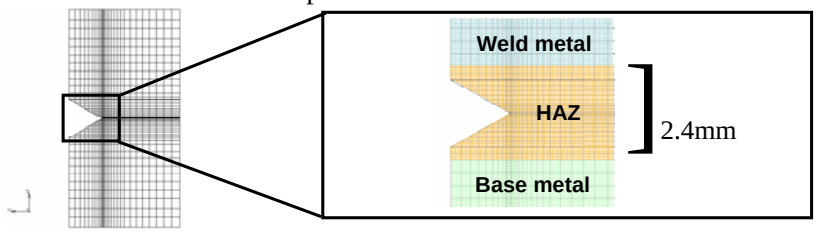

Fig. 14 The location of base metal, heat affected zone and weld metal for a circular notched specimen.

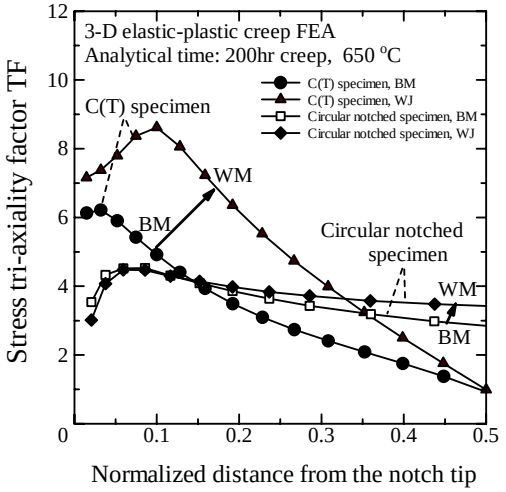

Fig. 15 The stress tri-axial factor TF of welded joint and base metal for C(T) and circular notched specimens.

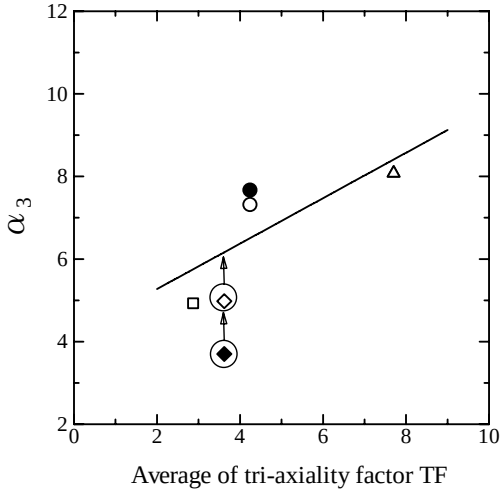

Fig. 16 Relationship between the value of α_3 and average value of TF.

5. Conclusions

1) The experimental characteristics of load line displacement for base metal and welded joint of C(T) and circular notched specimens were found to be characterized by the master curve for creep deformation based on the similarity law of creep deformation against the normalized time of stress application.
2) For base metal and welded joint of C(T) specimens, the values of α_3, which represent the accelerating creep deformation related to the creep ductility, were found to take constant independently of temperature. On the other hand, the values of α_3 for welded joint were found to increase with decrease in temperature, which result in the dependence of temperature.
3) The *QL** parameter, which is the estimating parameter of creep ductility, was found to show the good correlation with the α_3 and the stress tri-axial factor *TF*. Creep ductilty was found to be unified by *TF* near the crack tip and these are reflected in the value of α_3.

References

1. A. T. Yokobori Jr., R. Sugiura, M. Tabuchi, A. Fuji, T. Adachi and T. Yokobori: Proc. of Int. Conf. on Fracture (ICF11), (2005), CD-ROM.
2. T. Adachi, A. T. Yokobori Jr., M. Tabuchi, A. Fuji, T. Yokobori and K. Nikbin: *Mater. at High Temp.*, 21, 2 (2004), 95.
3. R. Sugiura, A. T. Yokobori Jr., M. Tabuchi, T. Yokobori: *Engng. Fract. Mech.*, 74 (2007), 868.
4. R. Sugiura, A. T. Yokobori Jr., K. Suzuki and M. Tabuchi: Proc. of Int. Conf. on Advan. Technol. in Experimental Mechanics 2007 (ATEM'07), JSME-MMD, Japan, (2007), CD-ROM
5. A. T. Yokobori Jr. and R. Sugiura: *Engng. Fract. Mech.*, 74 (2007), 898.
6. A. T. Yokobori Jr., T. Yokobori and M. Tabuchi, J. of Material Science, 31 (1996) 4746
7. A. T. Yokobori Jr., S. Takamori, T. Yokobori, Y. Hasegawa, K. Kubo and K. Hidaka, Key Engineering Materials, 171-174 (2000) 131
8. T. Fujita, K. Asakura, T. Sawada, T. Takamatsu and Y. Otoguro: *Metall. Trans. A*, 12A (1981), 1071.
9. T. Fujita: *Adv. Mater. & Processes*, 157, 6 (2000), 55.
10. M. Matsui, M. Tabuchi, T. Watanabe, K. Kubo and J. Kinugawa: *ISIJ Int.*, 41 (2001), S126.
11. T. Yokobori: Strength and materials, Iwanami, Japan, (1974), 110.
12. ASTM E1457-07. Standard Test Method of Measurement of Creep Crack Growth Rates in Metals, Annual Book of ASTM Standards, (2007).
13. T. Yokobori, T. Iwadate, S. Konosu, M. Tabuchi, A. Fuji, A. T. Yokobori Jr.: Strength of materials and fractology, 129 Committee of JSPS, Sasaki Press, Japan, (1999), 291.
14. H. H. Johnson: *Mater. Resea. and Stand.*, 5 (1965), 442.
15. K. H. Schwalbe and D. Hellmann: *J. of Test. and Eval*, 9, 4 (1980), 218.

16. R.E.Evans and B.Wilshire : Institue of metals, (1985), 197.
17. A. T. Yokobori Jr., T. Yokobori and K. Yamazaki: *J. of Mater. Sci. Letters*, 12 (1996), 2002.
18. A. T. Yokobori Jr. and M. Prager: *Mater. at High Temp.*, 10, 3 (1999), 137.
19. A.T.Yokobori Jr. and T.Yokobori: Advances in Fracture Research, Proc. of Int. Conf. on Fracture (ICF7), eds.by. K.Salama, K.Ravi-chandar, D.M.R.Taplin and P.Rama Rao, Pergamon Press, New York, (1989), 1723.
20. A. T. Yokobori Jr., T. Uesugi, T. Yokobori, A. Fuji, M. Kitagawa, I. Yamaya, M. Tabuchi and K. Yagi: *J. of Mater. Sci.*, 33 (1998), 1555.